DOI: 10.24996/ijs.2025.66.11.45

ISSN: 0067-2904

Novel Image Fusion Method for Brain Tumor Detection Using Gaussian Curvature and Edge-Preserving Filters

Srikanth M.V[1*], Nagasirisha B[2], P.Sarvana Kumar[3], E.Ramakrishna Reddy[1], A Suneel Kumar[1]

[1]*Usha Rama College of Engineering and Technology, Andhra Pradesh, India*
[2]*Gudlavalleru Engineering College, Andhra Pradesh, India*
[3]*SASI Institute of Technology & Engineering, Andhra Pradesh, India*

Received: 8/12/2024 Accepted: 18/8/2025 Published: 30/11/2025

Abstract

The process of combining images from multiple medical imaging sources while minimizing distortion and loss of information is known as medical image fusion. It improves the usefulness of medical imaging for diagnosing and treating medical issues by maintaining every feature in the fused image. Many image fusion techniques have been introduced recently, and significant progress has been made in medical diagnosis. However, the fusion performance of these contemporary methods may experience challenges such as distortion, noise, and blurring under certain conditions. To address these drawbacks of the current methods, this work presents a novel fusion methodology for enhanced visual clarity and detail retention. A new decomposition technique with an edge-preserving smoother was first described using Gaussian curvature and guided filters. The primary objective of this approach is to preserve edge haloes while recovering the structural information. The "weighted average" technique was used to merge source images based on the weights computed based on significant edge details. This technique can enhance contrast and highlight significant details in the fused image. The proposed methodology was evaluated on multiple publicly available medical imaging datasets. The quantitative evaluation indicates that the suggested fusion strategy for multimodal image fusion improves the average image entropy (IE) by 5.8, Mutual Information (MI) by 34.8%, Mean Structural Similarity Index Measure (MSSIM) by 31%, and Edge Strength (Q_{ABF}) by 40% over the current methods, demonstrating its potential applicability in clinical settings for accurate diagnosis.

Keywords: Gaussian curvature, Guided filter, Medical image fusion, Weighted average, Qualitative, Quantitative evaluation.

1. Introduction

Medical imaging serves as a fundamental basis for clinical decision-making in the medical journey of several patients. A wide range of clinical applications, including diagnosis, computer-assisted detection, treatment planning, action, and therapy, can use medical imagery. Medical imaging systems play a significant role in several clinical tasks. Still, the increasing demand for the practical interpretation of complex medical images suggests that reliable automated methods are required to alleviate the growing burden on healthcare professionals. Thus, Medical imaging science benefits from the development of advanced computational tools for analyzing medical images [1,2]. Innovation, particularly in

*Email: sree.02476@gmail.com

registration, segmentation, reconstruction, fusion, detection, modeling, and tracking, is being driven by the advancement of image capture, processing, and interpretation tools. Medical images often present challenges such as noise, artifacts, and modal variability, and demand prior knowledge to comprehend. Biomedical pictures can be noisy and contain many modality-specific artifacts depending on the acquisition settings and techniques. For more than two decades, research in medical image processing has diversified to include techniques such as segmentation, enhancement, and fusion. Initially, it concentrated on standard image analysis tasks, including segmentation, contrast enhancement, and registration. However, as medical image processing has developed, the domain of imaging biomarker identification has concentrated on converting functional data into pertinent biomarkers that can provide information about a range of medical disorders [3-6].

Information from several multimodal images of the same scene is combined in image fusion to create a single, cohesive image that is more detailed and clearer than the separate images. This study's main topic is multimodal medical image fusion, integrating images of the exact body location using techniques such as MRI, CT, PET, and SPECT. These medical pictures depict a variety of characteristics, including metabolic activity, bone structure, and other physiological specifics. Nonetheless, individual scans typically highlight specific features, such as structural details or metabolic activity. For example, MRI provides high-resolution structural details of soft tissues, while CT successfully distinguishes between tissues with varied densities, including blood arteries and bones.

In contrast, PET and SPECT have low spatial resolution but concentrate on metabolic and functional data. When combined, complementary qualities of these imaging modalities improve spatial resolution and combine important features into a single image, increasing diagnostic precision. These merged images help radiologists identify patients thoroughly and create efficient treatment plans.
Traditional image fusion techniques, such as Non-Subsampled Contourlet Transform (NSCT), Curvelet Transform (CVT), and Discrete Wavelet Transform (DWT), have been widely used [7-8]. Nevertheless, these techniques frequently struggle to combine intricate details from input imagery without adding artifacts. Deep learning approaches have become a potent tool in combining images with the introduction of machine learning, which has revolutionized the field [9]. In order to improve fusion quality in medical imaging, this work presents a novel multimodal image fusion technique that uses progressive information processing using Gaussian and guided filters. Numerous methods for fusing images have been proposed over time. Agarwal et al. [10] created a hybrid medical image fusion method incorporating wavelet transform and CVT. This technique produces high-quality fusion outputs with fewer errors by employing CVT to segment input images onto overlapping tiles and the wavelet transform to fuse sub-bands. A different method for multi-focus image fusion combines Principal Component Analysis (PCA) with Stationary Wavelet Transform (SWT) [11]. SWT breaks down images into smaller bands, but PCA-based algorithms prioritize important features, resulting in images that are clearer and free of artifacts.

Bavirisetti and Dhuli [12] suggested an edge-preserving fusion technique for visible and infrared pictures. In order to improve contrast and preserve important details, this technique uses anisotropic diffusion to decompose images as approximation and detail layers, which are then fused using the Karhunen-Loève transform using linear superposition. To minimize halo effects and preserve scale-specific details for more realistic fused images, another multiscale decomposition technique separates base and detail layers using Gaussian filtering and Rolling Guidance Filtering (RGF) [13]. Additionally, a rapid spatial filtering approach has been

presented [14], which evaluates image contrast with sharpness using gradient magnitude and then creates a weight map using morphological operations and structure-preserving filters. This procedure guarantees a natural-looking fused image. Lu et al. [15] suggested optimization methods based on linked matrix and tensor factorization for multimodal picture fusion, demonstrating improved reconstruction accuracy and noise resistance, as validated by specific metrics.

Techniques like Laplacian re-decomposition (LRD) overcome the drawbacks of conventional fusion methods, such as noise, blurring, and color distortion. LRD uses Laplacian decision graph decomposition for picture improvement, combining overlapping with non-overlapping domains to fuse complementary and redundant information efficiently. For low-resolution pictures, Dogra et al. [16] presented a multimodal fusion technique emphasizing ease of use and enhanced target detection for clinical applications. While Kumar and Joshi [17] used NSCT to split images into sub-bands and extract features using sophisticated inception models, Jose et al. [18] suggested an approach using Non-Subsampled Shearlet Transform (NSST) for applications like adolescent identification. This technique optimizes fusion decisions with multi-objective differential evolution, producing high-quality images by inverse transformation. This article presents a mechanism of image fusion using a novel image decomposition technique. The primary contributions of this work are as follows:
1. A novel method for image decomposition and extraction of detail layers of an image is presented.
2. Detail layers were utilized to create weight maps for images that will be fused depending on pixel significance.
3. Different benchmark datasets of brain tumors were used to evaluate the effectiveness of the suggested mechanism.

2. Concepts of Proposed Method

2.1 Guided Image Filter

A method known as the guided filter (GF), which smooths images while preserving edge information, analyzes the statistical properties of each pixel's immediate neighborhood to determine the output of the guided filter [19, 20]. This technique smooths the input image while maintaining the integrity of edge structures by connecting the output image to the guiding image using a local linear model. Within a square window w_k, with a guide image P centered at pixel k, the output F of the filter at pixel i can be expressed mathematically as follows:

$$F_i = m_k P_i + n_k \,, \forall i \in w_k \tag{1}$$

Where m_k, n_k are the coefficients that were computed using a local linear model within the window w_k that were used to minimize the defined objective function related to image smoothing and edge preservation as follows:

$$E(m_k, n_k) = \sum_{i \in w_k} (m_k P_i + n_k - I_i)^2 + \varepsilon m_k^2) \tag{2}$$

Where ε is the regularization control parameter. The optimal solution of equation (2) is given by the following values of m_k and n_k.

$$m_k = \frac{\frac{1}{|w|}\sum_{i \in w_k} P_i I_i - \mu_k E[I_k]}{\sigma_k^2 + \varepsilon} \tag{3}$$

$$n_k = E[I_k] - m_k \mu_k \tag{4}$$

Where |w| indicates the total count of pixels in w_k and μ_k, σ_k^2 are the mean and variance in w_k while $E[I_k]$ is the expectation of I in w_k. Once the linear coefficients were determined, Equation (1) can be used to solve for the output F_i ; however, pixel-

distinct windows share with overlaps w_k Centered at k. To solve this problem, use the filtered output from equation (5), which gives the average of all estimates of F_i.

$$F_i = \overline{m_i} P_i + \overline{n_i} \quad (5)$$

2.2 Algorithm to compute the Gaussian curvature of an Image

Step 1: Let I is the image whose Gaussian curvature is to be computed.

Step 2: Gaussian curvature of I is computed as follows:

(a) Obtain the smoothed image of I using equation (6)

$$I_s = Gaussian(I_1, 3) \quad (6)$$

Where $Gaussian$ is a function of 2D, defined as $(x, y, \sigma) = \frac{1}{2\pi\sigma^2} \exp\left(-\frac{x^2+y^2}{2\sigma^2}\right)$, with (x, y) representing the spatial coordinates of an image.

(b) Compute the first-order partial derivatives of I_s along x and y directions to get a gradient.

$$I_x = \frac{\partial I_s}{\partial x} \quad \text{and} \quad I_y = \frac{\partial I_s}{\partial y} \quad (7)$$

(c) Compute the second-order partial derivatives of I_s along x and y directions.

$$I_{xx} = \frac{\partial^2 I_s}{\partial x^2} \quad \text{and} \quad I_{yy} = \frac{\partial^2 I_s}{\partial y^2} \quad \text{and} \quad I_{xy} = \frac{\partial^2 I_s}{\partial x \partial y} \quad (8)$$

(d) Compute the Gaussian curvature (K) of an image using the following relation

$$K = \frac{I_{xx} I_{yy} - I_{xy}^2}{(1 + I_x^2 + I_y^2)^2} \quad (9)$$

The denominator $(1 + I_x^2 + I_y^2)^2$ normalizes the curvature based on the image gradient.

2.3 Proposed algorithm of Image fusion

Step 1: Read the Input images I_1 and I_2 that needs to be fused.

Step 2: Compute the Gaussian curvatures of I_1 and I_2 and label them as K_1 and K_2.

Step 3: By taking Gaussian curvatures as guidance images, smooth each source image using a guided filter.

$$I_{G1} = guided\ filter(I_1, K_1, r, \epsilon) \quad (10)$$

$$I_{G2} = guided\ filter(I_2, K_2, r, \epsilon) \quad (11)$$

Where r, ϵ are the size of the neighborhood and regularization parameters of the guided filter, which were taken as 15 and 0.01.

Step 4: Detail layers that capture significant intensity variations among pixels were obtained for each source image by subtracting the guided filter output from the respective source images.

$$I_{D1} = I_1 - I_{G1} \quad (12)$$

$$I_{D2} = I_2 - I_{G2} \quad (13)$$

Step 5: Compute the weight of each pixel of the detail layer in each source image based on their horizontal and vertical strength obtained from the Eigenvalues of the covariance matrix as described in equations (17) to (21).

$$W_1(p, q) = Horizontal\ strength\ of\ I_{D1}(p, q) + Vertical\ strength\ of\ I_{D1}(p, q \quad (14)$$

$$W_2(p, q) = Horizontal\ strength\ of\ I_{D2}(p, q) + Vertical\ strength\ of\ I_{D2}(p, q) \quad (15)$$

Where (p, q) specify the pixel locations, with each p and q varied from 1 to 256 for a 256x256 image.

Step 6: The fused image was computed by taking the weighted average of the source images using the weights W_1 and W_2

$$\text{Fused Image}, I_F(p, q) = \frac{(W_1(p,q) * I_1(p,q) + W_2(p,q) * I_2(p,q)}{(W_1(p,q) + W_2(p,q))} \quad (16)$$

The detailed flow diagram of the proposed fusion mechanism is illustrated in Figure 1.

2.4 Weight Computation Based on Pixel Significance

The weights were determined by using statistical characteristics of surrounding base coefficients [21]. In order to get the optimal weight, a square window of size NxN was taken into account around the surrounding area of the detail coefficients. $I_D(\mathrm{p},\mathrm{q})$. This neighborhood was treated as matrix A. By treating the row as an event and the column as a parameter of matrix A, equations (17) and (18) may be used to determine the covariance matrix of A and an unbiased estimate of its covariance matrix, $\mathrm{C_H^{p,q}(A)}$.

$$Covariance(A)) = E[(A - E[A])(A - E[A])^T \quad (17)$$

$$C_H^{p,q}(A) = \frac{1}{N-1}\sum_{z=1}^{N}(A_z - \bar{A})(A_z - \bar{A})^T \quad (18)$$

Where $\mathrm{A_z}$ indicates $\mathrm{z^{th}}$ observation of N-dimensional parameters while $\overline{\mathrm{A}}$ indicates its mean. It was determined that a vector of variances was provided for each column of matrix A by the diagonal elements of the matrix $\mathrm{C_H^{p,q}}$. The eigenvalues were calculated for the matrix $\mathrm{C_H^{p,q}}$, and the number of eigenvalues is exactly equal to the size of the matrix $\mathrm{C_H^{p,q}}$.The horizontal strength of the base coefficient at position (p,q) was described by the sum of all these Eigenvalues. Similarly, the vertical strength of the base coefficient at position (p,q) was described by the sum of all the Eigenvalues of the matrix $\mathrm{C_V^{p,q}}$, which is an unbiased estimate of the covariance matrix generated from the matrix by now treating the row as a parameter while treating the column as an event.

$$Horizontal\ strength\ (p,q) = \sum_{z=1}^{N} Eigen_z\ of\ C_H^{p,q} \quad (19)$$

$$Vertical\ strength\ (p,q) = \sum_{z=1}^{N} Eigen_z\ of\ C_V^{p,q} \quad (20)$$

By adding the $Horizontal\ strength\ and\ Vertical\ strength$, the overall weight W of the base coefficient at a location (p,q) can be estimated, which depends on the strengths of pixels and their intensity values

$$W(p,q) = Horizontal\ strength\ (p,q) + Vertical\ strength\ (p,q) \quad (21)$$

3. Results and Discussion

3.1 Subjective Analysis

Five MRI and CT scan datasets containing brain images, denoted as "Dataset-I" through "Dataset-V," were chosen to assess the efficacy of the suggested image fusion technique. These datasets consist of the following: sagittal perspective images of the brain as well as skull (Dataset-IV), a brain having cerebellar metastases (Dataset-V), a brain of a patient with fatal hemorrhage (Dataset-II), a brain that has neoplastic cancer (Dataset-III), and a healthy brain (Dataset-I). Every image was composed of 256 grayscale levels and measures 256 by 256 pixels. The Benchmark Atlas of the brain can be accessed at [http://www.med.harvard.edu/aanlib/home.html], where the datasets were obtained from [22].

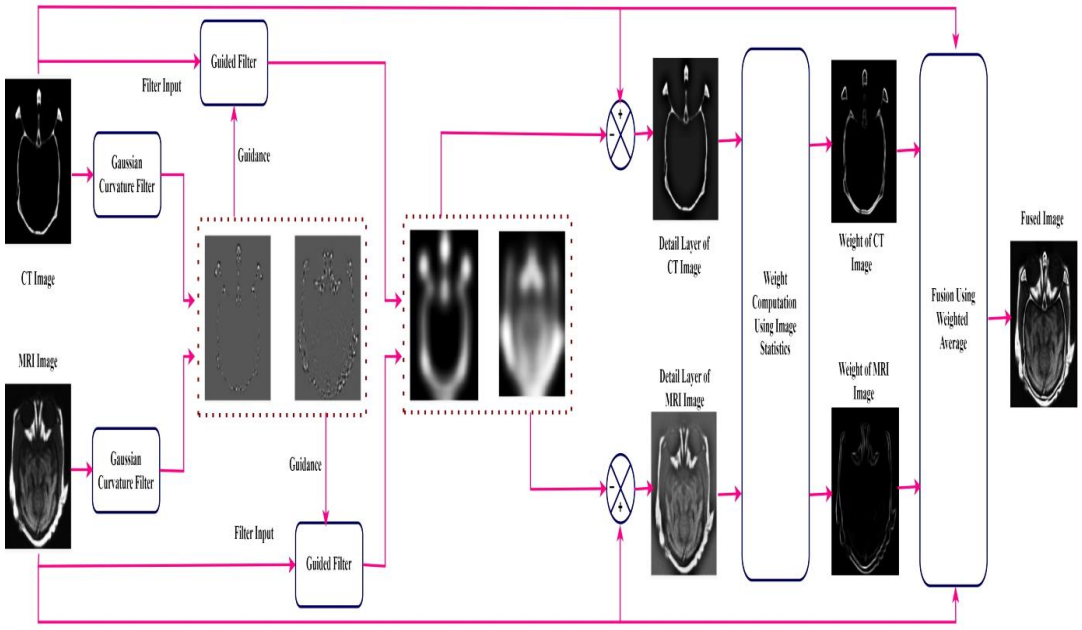

Figure 1: Process flow proposed fusion mechanism

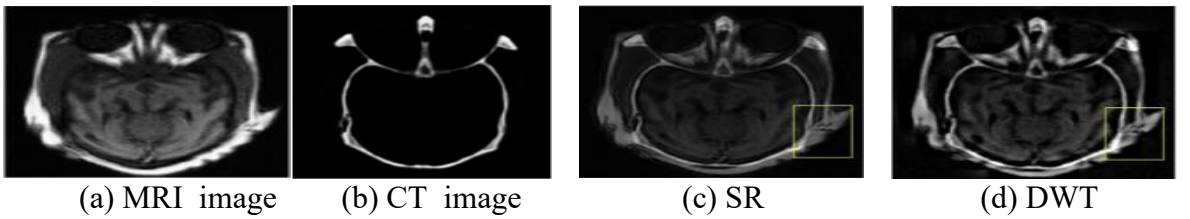

(a) MRI image (b) CT image (c) SR (d) DWT

(e) NSST (f) CNN (g) Guided filter (h) Proposed

Figure 2: Fused results of Dataset-I (CT-MRI of healthy brain)

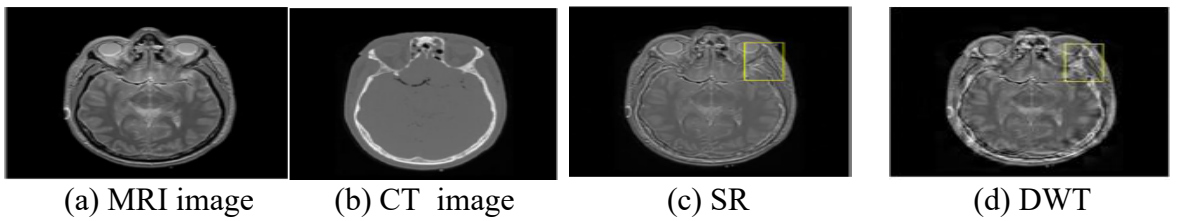

(a) MRI image (b) CT image (c) SR (d) DWT

(e) NSST (f) CNN g) Guided filter (h) Proposed

Figure 3: Fused results of Dataset-II (CT-MRI of Fatal stroke)

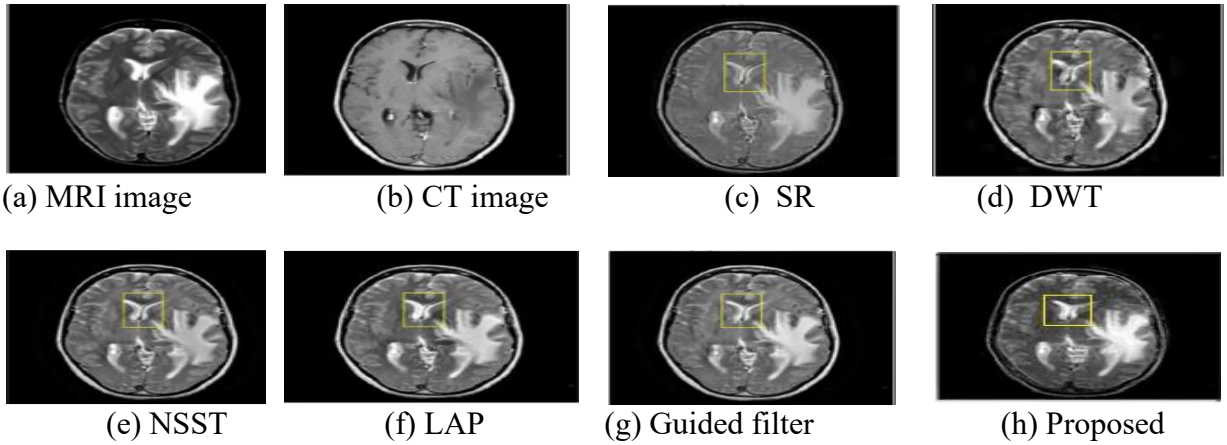

Figure 4: Fused results of Dataset-III (CT-MRI of neoplastic tumor)

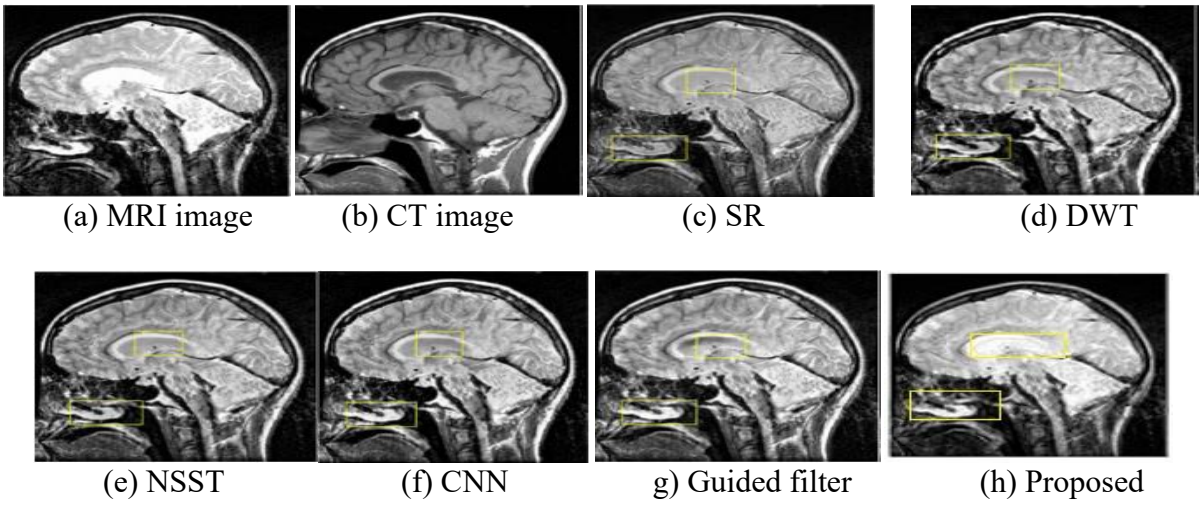

Figure 5: Fused results of Dataset-IV (CT-MRI of brain skull)

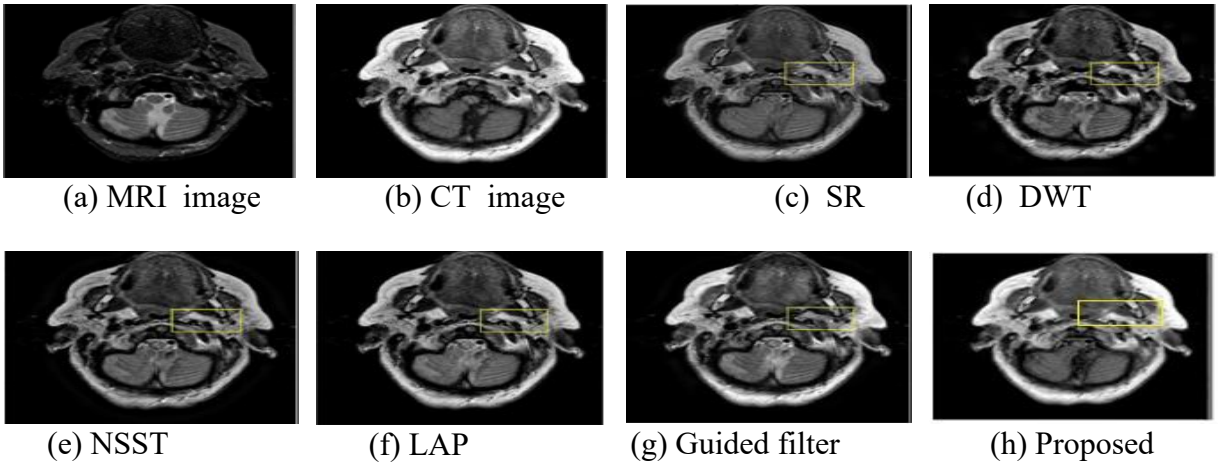

Figure 6: Fused results of Dataset-V (CT-MRI of Cerebella metastasis)

Figure 2 displays the fusion findings for Dataset-I, with corresponding MRI and CT images in Figs. 2(a) and (b). The results of various fusion strategies are presented in Figs. 2(c) through (h), including guided filter approaches, the suggested method, Convolutional

Neural Network (CNN), Sparse Representation (SR), Discrete Wavelet Transform (DWT), and Non-Subsampled Shearlet Transform (NSST). Although the connective tissue details obtained through the MRI and the skeletal structure from the CT were generally preserved, there were observable differences in the preservation of detail and contrast across the modalities. A yellow rectangle highlights the distinctions between the various fusion techniques. The fused images, as displayed in Figs. 2(c) and (d) reveal a slightly faint brightness in the highlighted area. However, information on the CT image is typically preserved in the NSST and CNN fusion images, as seen in Figs. 2(e) and (f), but certain data from the MRI image is typically lost. Compared to the suggested approach, which can retain every aspect of the original image, the guided filter's visual clarity is equivalent. The contrast of the guided filter was weaker than that of the proposed method, as seen in Figs. 2(g)–(h). Dataset-II is the second set of medical images, and Fig. 3 shows the fusion results.

As seen in Fig. 3(d), using DWT leaves hard tissues, including bone structures, with little visual impact and information. This low contrast issue is shown in Fig. 3(c). The other three methods currently in use produced results that were not significantly different. The suggested approach finds capturing pixel intensity fluctuations throughout rows and columns in CT scans challenging, which results in a lower retention of CT information than the guided filter. A third clinical dataset (Dataset-II) was used in Figure 4(h) to compare the suggested method with alternative methodologies. The fused image generated through the recommended process exhibits strong contrast and meticulous preservation of soft tissue detail. Fusion results for Datasets IV and V are shown in Figures 5 and 6. Techniques like NSST, DWT, and SR do not accurately depict bone structures or retain important information from the original pictures [23]. Conversely, the suggested approach demonstrates improved performance, as indicated by higher scores in key evaluation metrics.

3.2 Objective Analysis

Qualitative and quantitative evaluation criteria must be applied to measure fusion performance. In this paper, various fusion processes were assessed for their effectiveness using quantitative assessment measures such as standard deviation (SD), mutual information (MI), image entropy (IE), spatial frequency (SF), mean structural similarity (MSSIM), and margin information retention (Q_{ABF}). Table 1 presents an explanation of these measurements. Standard Deviation (SD), Mutual Information (MI), Spatial Frequency (SF), Image Entropy (IE), Edge Strength (Q_{ABF}), and Mean Structural Similarity Index Measure (MSSIM) were six commonly used metrics that were used to assess the quantitative performance of different image fusion techniques across five benchmark datasets.

Table 1: Formulae and significance of image quality assessment metrics

Performance Metric	Mathematical formulae
Average Pixel Intensity (API)	For an image $f(i,j)$ of size MXN, $API = \frac{1}{MN}\sum_{i=1}^{M}\sum_{j=1}^{N} \mathrm{f}(i,j)$ A higher value of API produces an image with more contrast.
Standard Deviation (SD)	It is a metric for the level of deviation in a mean collection of image data. $\mathrm{SD} = \sqrt{\frac{1}{\mathrm{MN}}\sum_{\mathrm{i-1}}^{\mathrm{M}}\sum_{\mathrm{j=1}}^{\mathrm{N}}(\mathrm{f(i,j)} - \mathrm{API})^2}$
Entropy (IE)	It estimates the information content in an image. A larger value of H indicates a greater amount of information content within the image. For an image with a probability of pixel intensity distribution $\mathrm{P_k}$, entropy was calculated as follows: $\mathrm{H} = -\sum_{\mathrm{k=0}}^{255} \mathrm{P_k} \log(\mathrm{P_k})$
Mutual Information (MI)	For two source images A, B, and the fused image F , the Mutual information is given as $MI_F^{AB} = MI(A,F) + MI(B,F)$ $MI(A,F) = \sum_{z\in Z}\sum_{y\in Y} p(A,F) log_2 \frac{p(A,F)}{p(A)p(F)}$ $\mathrm{MI}(B,F) = \sum_{z\in Z}\sum_{y\in Y} p(B,F) log_2 \frac{p(B,F)}{p(B)p(F)}$ The quantity of activity-level data transmitted from the source images into the fused image was measured.
Spatial Frequency (SF)	It measures the resolution level of an image. A higher value was typically preferred for improved image quality. $SF(i,j) = \sqrt{\lvert RF(i,j)\rvert^2 + \lvert CF(i,j)\rvert^2}$ $RF(i,j) = \sqrt{\frac{1}{MxN}\sum_{i=2}^{M}\sum_{j=2}^{N}[I(i,j) - I(i,j-1)]^2}$ $CF(i,j) = \sqrt{\frac{1}{MxN}\sum_{i=2}^{M}\sum_{j=2}^{N}[I(i,j) - I(i-1,j)]^2}$
Edge Strength ((Q_{ABF}))	Q_{ABF} represents the degree to which the edge information from the input images transitions into the fused image. The evaluation is as follows: $Q_{ABF} = \frac{\sum_{i=1}^{M}\sum_{j=1}^{N}(Q_{AF}(i,j)W_A(i,j) + Q_{BF}(i,j)W_B(i,j))}{\sum_{i=1}^{M}\sum_{j=1}^{N}(W_A(i,j) + W_B(i,j))}$
Mean Structural Similarity Index Measure (MSSIM)	$SSIM(A,F) = \frac{(2\mu_A\mu_F + C1)(2\sigma_{AF} + C2)}{(\mu_A{}^2 + \mu_F{}^2 + C1)(\sigma_A{}^2 + \sigma_F{}^2 + C2)}$ The variance of A is represented by $\sigma_A{}^2$, the variance of F by $\sigma_F{}^2$, the covariance of A and F by σ_{AF}, and the mean of A and F by μ_A and μ_F, respectively. Using two constants, $C1$ and $C2$, prevents the instability that can arise from a division with a value close to zero. SSIM readings are between 0 and 1, where 1 denotes exceptional quality and 0 denotes poor quality. Less distortion is present in the fused image when the MSSIM score is greater. $MSSIM = \frac{SSIM(A,F) + SSIM(B,F)}{2}$

The results are summarized in Table 2. To make direct comparison easier, the best values for each dataset were bolded. As demonstrated by its persistent superior results in MI, IE, Q_{ABF}, and MSSIM, the suggested fusion method is successful at acquiring and retaining important structural and visual information from the source images. The increased information richness and decreased redundancy of fused output are indicated by larger Image Entropy, while increased Mutual Information specifically shows a stronger preservation of complementary information from both modalities. The enhanced Q_{ABF} values further support the method's ability to preserve edge details with more accuracy. This is crucial in healthcare and satellite images, in which boundary precision is essential. The structural integrity and

perceived coherence of the fused results are highlighted by the high MSSIM ratings, which are close to 1 across datasets. On the other hand, metrics such as SF and SD, which are mostly related to texture sharpness and intensity fluctuation, display relatively similar values among techniques. This implies that although conventional methods might preserve fundamental levels of contrast and detail, they are unable to successfully incorporate the semantic and perceptual quality of the input images, whereas the suggested method performs better.

The average values of the four most important metrics (MI, IE, Q_{ABF}, and MSSIM) calculated over 30 typical slices from each of the five datasets are shown in Figure 7. The suggested approach continuously outperforms current methods, such as transform-based approaches (Discrete Wavelet Transform (DWT), Non-subsampled Shearlet Transform (NSST)), deep learning models (Convolutional Neural Networks (CNN)), and filtering strategies (Guided Filter), as the graphical comparison confirms. Notably, the suggested approach more successfully preserves information substance, clarity, and structure across a variety of fusion scenarios.

Table 2: Statistical evaluation of a proposed method for multimodal datasets

Dataset type	Method	Standard Deviation (SD)	Mutual Information (MI)	Spatial Frequency (SF)	Image Entropy (IE)	Edge Strength (Q_{ABF})	MSSIM
Dataset-I	SR	30.82	2.57	11.68	5.80	0.5756	0.5122
	DWT	44.71	1.92	17.13	6.17	0.6073	0.5246
	NSST	44.16	2.05	17.05	6.20	0.6816	0.5366
	CNN	52.89	2.43	17.40	6.07	0.7184	0.5518
	Guided filter (GF)	52.89	2.31	16.97	6.52	0.7210	0.5634
	Proposed	**57.79**	**4.43**	**21.00**	**6.80**	**0.9093**	**0.9922**
Dataset-II	SR	51.40	3.42	17.76	4.94	0.5178	0.8248
	DWT	55.73	3.19	22.01	5.19	0.5051	0.7915
	NSST	54.56	3.34	20.95	5.12	0.5887	0.8160
	CNN	59.92	3.34	21.93	4.89	0.5888	0.8146
	Guided filter (GF)	55.68	3.79	20.25	**5.20**	0.6028	0.8207
	Proposed	**59.05**	**4.76**	**21.48**	4.82	**0.8467**	**0.9941**
Dataset-III	SR	61.50	3.18	20.19	4.52	0.5157	0.7640
	DWT	66.53	3.12	25.11	4.86	0.5473	0.7489
	NSST	65.89	3.20	24.52	4.88	0.5971	0.7733
	CNN	69.60	3.38	25.99	4.39	0.6042	0.7775
	Guided filter (GF)	69.63	3.34	24.39	5.05	0.6119	0.7762
	Proposed	**71.03**	**4.26**	**26.75**	**5.28**	**0.8363**	**0.9807**
Dataset-IV	SR	69.84	3.33	28.98	7.56	0.4964	0.6532
	DWT	76.80	3.08	35.94	7.41	0.4699	0.6263
	NSST	79.49	3.23	34.60	7.44	0.5349	0.6628
	CNN	79.84	3.26	32.85	7.31	0.5171	0.6462
	Guided filter (GF)	75.36	3.52	34.30	7.60	0.5510	0.6602
	Proposed	**83.15**	**4.01**	**36.86**	**7.65**	**0.8631**	**0.9818**
Dataset-V	SR	51.71	3.19	17.58	5.24	0.4823	0.7427
	DWT	55.72	2.80	22.28	5.36	0.4573	0.7098
	NSST	53.79	2.94	21.47	5.44	0.5226	0.7311
	CNN	61.11	3.18	23.06	4.83	0.5214	0.7448
	Guided filter (GF)	66.98	3.23	21.56	5.60	0.5330	0.7342
	Proposed	**72.91**	**4.20**	**26.07**	**5.62**	**0.8686**	**0.9895**

4. Result Analysis

According to the experimental results, low intensity and a lack of bone structural knowledge lead to suboptimal fusion performance for (DWT) and Sparse Representation (SR) methods. NSST and CNN do not effectively preserve textures and edges in the yellow-highlighted area and guided filter techniques, although they produce a respectable visual impression. On the other hand, the suggested technique successfully preserves critical features of soft tissues and bone structure, leading to brighter and more vibrant fused images. Standard deviation (SD), image entropy (IE), and spatial frequency (SF) are three of the six metrics considered for evaluation. These metrics are frequently used to evaluate the quality of fused images and identify intrinsic image features. IE measures the data entropy of the fused image, SD indicates its contrast, and SF reflects its clarity. Higher SD values indicate a wider gray-level distribution, which enhances contrast of the fused image. Current approaches often include irrelevant details that artificially inflate these metrics.

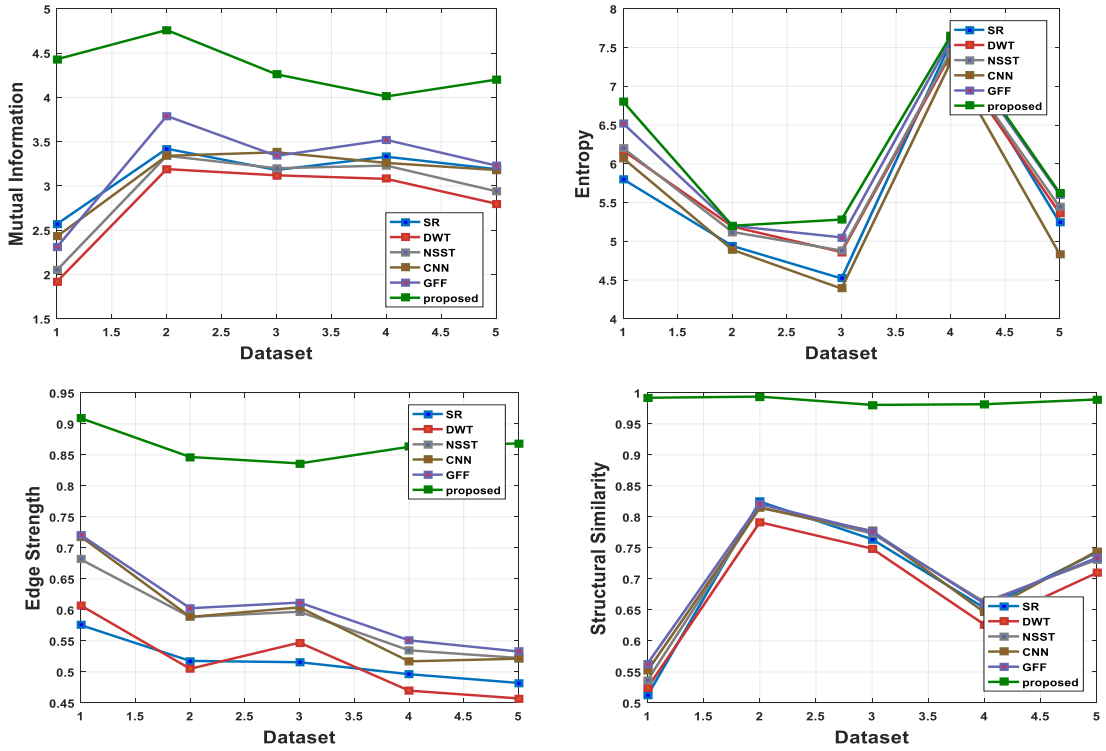

Figure 7: Comparative evaluation of the average value of quality assessment metrics

Three new metrics—Q_{ABF}, MSSIM, and MI—are introduced in this study to allow for a more thorough objective assessment. In order to determine the quantity of information retrieved, MI compares the pixel gray level distributions of the source image pair. MI rises with the extraction of additional features and the increased clarity and activity of the fused image. The source images' translation of edge information, including texture and hard structures, into the fused output was evaluated by $Q_{AB/F}$, whereas MSSIM measures the degree of distortion in the fused image. This metric becomes crucial in clinical applications since larger values allow for more precise pathological evaluations based on edge details. When compared to current methods, the suggested algorithm increases mutual information by 34.8%, image entropy by up to 5.8%, spatial frequency by about 27%, mean deviation by 22.8%, the structural similarity value by 31%, and edge sharpness by 40% compared to other methods, according to statistical evaluation of experimental results. These enhancements

show that the fused image has little distortion and a suitable balance of dense structures, soft tissue details, prominent features, and important edge information.

5. Conclusion

This work presents a novel image decomposition technique for image fusion using a Gaussian curvature filter and guided filter. In the proposed method, important details from the source images are more efficiently extracted, and the weight of these details in the original images was then calculated using image statistics. Utilizing the weighted average approach, source images were combined to produce the fused image. The effectiveness of the suggested method was validated through multiple comparative studies on CT and MR images. Further research could look into various enhancements, such as incorporating deep learning-based decomposition techniques or adaptation to optimize the real-time extraction of relevant information. The method's versatility for therapeutic and diagnostic applications could be increased by expanding it to incorporate additional imaging modalities or modifying it for real-time fusion.

References

[1] N.Liang, "Medical image fusion with deep neural networks," *Scientific Reports*, vol. 14, article no. 7972, April 2024. https://doi.org/10.1038/s41598-024-58665-9

[2] T. Zhou, QianRu Cheng, HuiLing Lu, Qi Li, XiangXiang Zhang and Shi Qiu, "Deep learning methods for medical image fusion: A review," *Computers in Biology and Medicine*, vol. 160, June 2023.https://doi.org/10.1016/j.compbiomed.2023.106959.

[3] R.Irfan, A.A.Almazroi, H.T.Rauf, R.Damaševičius, E.A.Nasr and A.E.Abdelgawad, "Dilated Semantic Segmentation for Breast Ultrasonic Lesion Detection Using Parallel Feature Fusion," *Diagnostics*, vol.11, no.7, July 2021.

[4] P. Velliangiri, I.T.Joseph and S.A.P.Kumar, "Investigation of Deep Learning Schemes in Medical Application," *International Conference on Computational Intelligence and Knowledge Economy (ICCIKE)*, Dubai, United Arab Emirates, pp. 87-92, 2019.

[5] M.I.Sharif, M.A.Khan, M.Alhussein, K. Aurangzeb and M.Raza, "A decision support system for multimodal brain tumor classification using deep learning," *Complex & Intelligent Systems*, vol.8, pp.3007–3020,2022.

[6] A. Stadlbauer, K.Nikolic, S.Oberndorfer, F.Marhold, T.M.Kinfe, A.M.Base, D.A.Bistrian, O.Schnell and A.Doerfler, "Machine Learning-Based Prediction of Glioma IDH Gene Mutation Status Using Physio-Metabolic MRI of Oxygen Metabolism and Neovascularization," *Cancers*, vol.16, no.6, Mar 2024.

[7] M. B. Abdulkareem, "Design and Development of Multimodal Medical Image Fusion using Discrete Wavelet Transform," *Second International Conference on Inventive Communication and Computational Technologies (ICICCT),* Coimbatore, India, pp. 1629-1633, 2018. doi: 10.1109/ICICCT.2018.8472997.

[8] S. Ibrahim, M.A.Makhlouf and G.El-Tawel, "Multimodal medical image fusion algorithm based on pulse coupled neural networks and nonsubsampled contourlet transform," *Medical & Biological Engineering & Computing*, vol.61, pp.155–177,2023.

[9] H. Zhang, H. Xu, X. Tian, J. Jiang and J. Ma, "Image fusion meets deep learning: A survey and perspective," *Information Fusion*, vol. 76, pp.323-336, 2021.

[10] J. Agarwal and S. S. Bedi, "Implementation of hybrid image fusion technique for feature enhancement in medical diagnosis," *Human-centric Computing and Information Sciences*, vol. 5, article no. 3, 2015. https://doi.org/10.1186/s13673-014-0020-z

[11] A.A. Abdullatif, A.F.Abdullatif and Amna al Safar, "Multi-Focus Image Fusion Based on Stationary Wavelet Transform and PCA on YCBCR Color Space," *Journal of Southwest Jiaotong University*, vol. 54, no.5, 2019.

[12] D. P. Bavirisetti and R. Dhuli, "Fusion of infrared and visible sensor images based on anisotropic diffusion and Karhunen-Loeve transform," *IEEE Sensors Journal*, vol. 16, no. 1, pp. 203-209, 2015.

[13] L. Yan, J. Cao, S. Rizvi, K. Zhang, Q. Hao and X. Cheng, "Improving the Performance of Image Fusion Based on Visual Saliency Weight Map Combined With CNN," *IEEE Access*, vol. 8, pp. 59976-59986, 2020.

[14] Z. Fu, Y. Zhao, Y. Xu, L. Xu and J. Xu, "Gradient structural similarity based gradient filtering for multi-modal image fusion," *Information Fusion*, vol. 53, pp. 251-268, 2020.https://doi.org/10.1016/j.inffus.2019.06.025.

[15] L. Lu, X. Ren, K. H. Yeh, Z. Tan, and J. Chanussot, "Exploring coupled image fusion based on joint tensor decomposition," *Human-centric Computing and Information Sciences*, vol. 10, article no. 10, 2020. https://doi.org/10.1186/s13673-020-00215.

[16] A.Dogra and S.Kumar, "Multi-modality medical image fusion based on guided filter and image statistics in multidirectional shearlet transform domain," *Journal of Ambient Intelligence and Humanized Computing*, vol. 14, pp.12191–12205, 2023. https://doi.org/10.1007/s12652-022-03764-6

[17] V. Kumar, K.Joshi, Rajesh Kumar, A. Harishchander, B.Vivek Kumar, B.Dev, A.Tripathi and M. Minakshi, "Multi Modalities Medical Image Fusion Using Deep Learning and Metaverse Technology: Healthcare 4.0 A Futuristic Approach," *Biomedical and Pharmacology Journal*, vol. 16, issue 4, 2023.

[18] J. Jose, N.Gautam, M.Tiwari, T.Tiwari, A.Suresh, V.Sundararaj and M.R.Rejeesh, "An image quality enhancement scheme employing adolescent identity search algorithm in the NSST domain for multimodal medical image fusion," *Biomedical Signal Processing and Control*, vol. 66, April 2021.

[19] S. Li, X. Kang and J. Hu, "Image Fusion With Guided Filtering," *IEEE Transactions on Image Processing*, vol. 22, no.7, pp. 2864-2875, July 2013. doi: 10.1109/TIP.2013.2244222.

[20] H. Zhang, X. Han and R. Zhang, "Multimodal Image Fusion Method Based on Guided Filter," *International Journal of Pattern Recognition and Artificial Intelligence*, vol. 36,no.1, 2022. https://doi.org/10.1142/S0218001422540039

[21] B.K.Shreyamsha Kumar, "Image fusion based on pixel significance using cross bilateral filter," *Signal, Image and Video Processing*, vol.9, pp. 1193–1204,2015.

[22] K.A. Johnson, J.Alex Becker, "The whole brain atlas," [Online]. Available: http://med.harvard.edu/aanlib/home.html.

[23] S. M.V., S. Kethavath, S. Yerram, S. Kalli, Nagasirisha and B, J. Brahmaiah Naik, "Brain Tumor Detection through Image Fusion Using Cross Guided Filter and Convolutional Neural Network," *ECTI-CIT Transactions*, vol. 18, no. 4, pp. 579–590, Oct. 2024.